

Preparation of solid polymer electrolyte composites: investigation of the precipitation process

P. MILLET

Laboratoire des Composés Non Stoechiométriques, Université de Paris-Sud, Bât. 415, 91405 Orsay Cedex, France

F. ANDOLFATTO, R. DURAND

Centre de Recherche en Electrochimie Minérale et en Génie des Procédés, BP 75, 38402 Saint-Martin d'Hères Cedex, France

Received 2 June 1994; revised 15 September 1994

A model for the chemical reduction of platinum tetramine in perfluorinated Nafion[®] membranes using sodium borohydride as reducer is proposed. A Nernst–Planck equation is employed for the description of ion transport by diffusion and migration and a reaction term accounts for the *in situ* chemical reduction. Time-dependent concentrations of the diffusing species within the membrane are obtained numerically by an iterative technique until completion of the precipitation. The model assumes that mass transport is limited by diffusion and migration within the membrane and that the concentrations remain constant at the interfaces during the precipitation. The model shows the effect of (i) the reducer concentration in the solution, (ii) the number of precipitation cycles and (iii) the rate of chemical reduction. To check the validity of the model, metallic platinum concentration profiles across the membrane thickness are obtained by electron microprobe analysis. Values of the diffusion coefficients of the diffusing species within the membrane are obtained from conductivity and permeation measurements.

List of symbols

C_b^0	reducer concentration in the bulk solution (mol cm ⁻³)	k	Boltzmann constant (1.38×10^{-23} J K ⁻¹)
C^-	sulfonate concentration in the membrane (mol cm ⁻³)	M_{Pt^0}	platinum molecular weight (kg mol ⁻¹)
C_i	concentration in species i in the Nafion [®] membrane (mol cm ⁻³)	R	perfect gas constant (8.32 J kg ⁻¹ K ⁻¹)
D_i	diffusion coefficient of species i in the membrane (cm ² s ⁻¹)	T	absolute temperature (K)
EME	electrode-membrane-electrode unit	u_i	absolute ionic mobility of species i (cm ³ s ⁻¹ J ⁻¹)
e	thickness of EME unit (cm)	V	membrane volume (cm ³)
F	Faraday (96 500 C mol ⁻¹)	z_i	charge beared by species i
		Φ_i	flux of species i (mol cm ⁻² s ⁻¹)
		ϕ	electric potential (V)
		Σ	constant defined by Equation 12
		τ	empirical factor varying from 1 to 0 and used to account for different chemical reactivities

1. Introduction

The preparation of platinum-based Nafion[®] composites is of practical interest because of potential applications in solid polymer electrolyte (SPE[®]) water electrolyzers and hydrogen/oxygen fuel cells.

In the literature, several methods have been reported for the plating of platinum electrodes [1–4]. Since the mid-1980s we have developed a procedure based on localized chemical reduction of cationic noble-metal salts into Nafion[®] membranes [5, 6]. The procedure consists of (i) ion-exchanging the Nafion[®] membrane initially in the H⁺ form with platinum tetramine, and (ii) reducing *in situ* the

platinum salt near the membrane surface. Sodium borohydride is usually used as reducing agent. The electrochemical performances of the membrane-electrode assemblies (MEAs) thus obtained are directly related to the metallic platinum distribution across the membrane thickness.

Initially, the best conditions for the preparation of the composites were determined empirically [7]. These conditions obtained, for samples of up to 5 cm², were found inappropriate for the preparation of larger samples. Therefore, a better understanding of the phenomena controlling the precipitation and the distribution of metallic particles inside the membrane was needed. Experimental data relative to the ion-exchange and precipitation processes were

collected using EXAFS (extended X-ray absorption fine structure) spectroscopy in dispersive mode and electron microprobe analysis [8]. In addition to the kinetic information on the ion-exchange and precipitation processes, it was shown that platinum tetramine incorporates the membrane in the form $[\text{Pt}(\text{NH}_3)_4]^{2+}$. The ion-exchange process was found to be rate controlled by diffusion of the ions either across a diffusion layer adjacent to the membrane surface or in the membrane itself [9], depending on the experimental conditions.

In this paper, we consider the *in situ* reduction of the tetramine salt in the Nafion[®] membrane. The precipitation is described by using phenomenological equations of mass transport and by taking into account the effect of the electric field on diffusion. Platinum concentration profiles across the membrane were computed until completion of the precipitation. The validity of the model was checked using data obtained by electron microprobe analysis [7]. Values of the diffusion coefficients within the membrane were deduced from resistivity measurements assuming the validity of the Einstein equation between absolute ionic mobility and self diffusion coefficient.

2. Experimental details

2.1. Materials

Perfluorosulfonic acid polymer sheets (Dupont de Nemours Nafion[®] products) were used as membranes. Nafion[®] 117 (equivalent weight 1100 g mol^{-1} and dry thickness 0.178 mm) was chosen because of its commercial availability. Before electrode deposition, a two-step standard procedure of cleaning was followed for every sample: (i) immersion for 30 min in boiling $\text{HNO}_3\text{-H}_2\text{O}$ (1:1 vol) solution to remove impurities; (ii) immersion for 1 h in boiling deionised water (resistivity of $18 \text{ m}\Omega \text{ cm}$ at 20° C) to introduce a reproducible amount of water into each sample [8]. Platinum tetramine ($[\text{Pt}(\text{NH}_3)_4]\text{Cl}_2 \cdot \text{H}_2\text{O}$) and sodium borohydride (NaBH_4) were purchased from Johnson Matthey and Merck, respectively.

2.2. Diffusion coefficients in the membrane

Platinum precipitation in the Nafion[®] membrane can be described simply by considering the diffusion of Na^+ , BH_4^- and $[\text{Pt}(\text{NH}_3)_4]^{2+}$. Values of the diffusion coefficients for Na^+ and $[\text{Pt}(\text{NH}_3)_4]^{2+}$ in Nafion[®] 117 membranes were obtained as detailed elsewhere [10]. Briefly, they were deduced from conductivity measurements, assuming the validity of the Einstein relation between self diffusion coefficient and absolute ionic mobility. Ionic conductivities of the ion-exchanged samples in Na^+ and $[\text{Pt}(\text{NH}_3)_4]^{2+}$ forms were measured using a mercury cell. The following values of the diffusion coefficient were

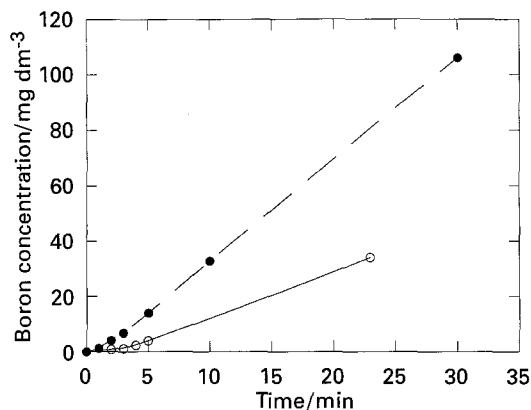


Fig. 1. Boron concentration against time measured in the right hand compartment of a permeation cell. The membrane is a Nafion[®] 117 hydrated perfluorosulfonated sheet. Boron concentration in the left compartment is (○) $1 \times 10^{-3} \text{ mol cm}^{-3}$ and (●) $2 \times 10^{-3} \text{ mol cm}^{-3}$.

obtained:

$$D_{\text{Na}^+} = 4.5 \times 10^{-6} \text{ cm}^2 \text{ s}^{-1}$$

$$D_{[\text{Pt}(\text{NH}_3)_4]^{2+}} = 5.2 \times 10^{-7} \text{ cm}^2 \text{ s}^{-1}$$

The value of $D_{\text{BH}_4^-}$ was deduced from permeation measurements. A sodium exchanged Nafion[®] membrane (5.31 cm^2) was mounted in a two-compartment cell. The left hand compartment was filled with a $10^{-3} \text{ mol cm}^{-3}$ NaBH_4 solution and the right hand compartment with pure water. Every two minutes, 1 cm^3 of the solution was taken from the right hand compartment for analysis (flame spectroscopy). The boron concentration was then plotted as a function of time (Fig. 1). From the slope of the curve in the steady state, the global diffusion coefficient for NaBH_4 was determined: $D_{\text{NaBH}_4} = 4.9 \times 10^{-7} \text{ cm}^2 \text{ s}^{-1}$.

Using the transport model described below for steady state diffusion and knowing the value of D_{Na^+} , $D_{\text{BH}_4^-}$ was adjusted to fit the experimental permeation data. A value of $D_{\text{BH}_4^-} = 5 \times 10^{-7} \text{ cm}^2 \text{ s}^{-1}$ was obtained. This value which is close to the global diffusion coefficient for NaBH_4 indicates that the effect of the electric field on diffusion remains negligible during the transport process. By comparison, the diffusion coefficient of hydroxyl ions inside a Nafion[®] membrane of the same equivalent weight was obtained by permeation measurements [11]. Its value was $6.0 \times 10^{-7} \text{ cm}^2 \text{ s}^{-1}$.

2.3. Measurements of platinum concentration profiles

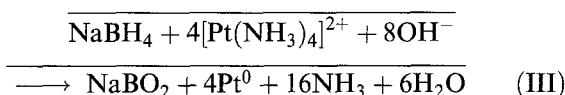
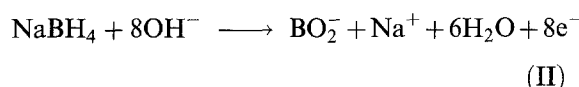
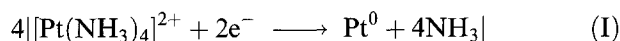
$[\text{Pt}(\text{NH}_3)_4]^{2+}$ exchanged Nafion[®] 117 samples (geometrical area $\sim 1 \text{ cm}^2$) were immersed for 2 h in 50 cm^3 NaBH_4 aqueous solutions of various concentration ($2.5 \times 10^{-5} - 2 \times 10^{-3} \text{ mol cm}^{-3}$). The solutions were stirred using a magnetic stirrer. Once the precipitation was completed, the samples were thoroughly washed with water, air-dried and embedded in resin. Metallic platinum concentration profiles across the membrane were then obtained using a Camebax electron microprobe analyser. The graphs were then normalized to account for the significant change in the membrane volume (25%)

which occurs during the drying process (dry thickness 178 μm , hydrated thickness 200 μm).

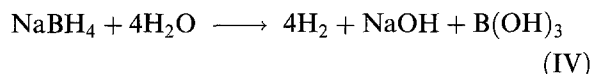
3. Theory

3.1. The reduction process

The chemical reduction of platinum tetramine inside the membrane occurs, according to [12], as follows:



The hydroxyl ions required for the reaction are produced by the decomposition of NaBH_4 according to



Reaction stoichiometry is such that nine moles of NaBH_4 are required for the reduction of four moles of $[\text{Pt}(\text{NH}_3)_4]^{2+}$. One NaBH_4 is used for the reduction and the other eight fuel the reaction with hydroxyl ions.

Reaction IV may cause a depletion in NaBH_4 . In fact, an equilibrium is rapidly reached when the pH of the solution is ~ 11 . At room temperature, the rate of decomposition of NaBH_4 is $1.0 \times 10^{-7} \text{ mol s}^{-1} \text{ dm}^{-3}$ (Fig. 2). With these values, after 2 h, a $7.5 \times 10^{-5} \text{ mol cm}^{-3}$ NaBH_4 solution loses only 1% of its initial concentration. The rate of decomposition is increased by a factor two in the presence of finely divided platinum. The pH of the solution had a constant value of ~ 11 . The pH inside the membrane was alkaline but was not measured.

3.2. Determination of the mass transport mechanism

The reduction process may be limited by any of the three limiting rates: (a) diffusion in the boundary layer is rate-determining (L mechanism), (b) diffusion in the membrane is rate-determining

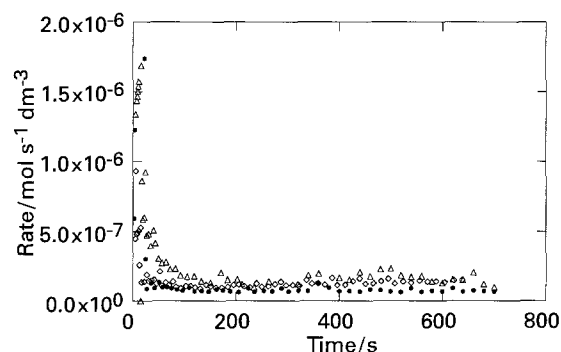


Fig. 2. Rate of decomposition of sodium borohydride in stirred solutions (stirrer speed: 350 rpm) at room temperature. Key: (○) 1.00×10^{-3} , (●) 3.75×10^{-4} and (△) $7.50 \times 10^{-5} \text{ mol cm}^{-3}$.

(M mechanism) and (c) chemical reduction is rate-determining (R mechanism).

If the R mechanism were rate-determining, the $\text{Na}^+ - [\text{Pt}(\text{NH}_3)_4]^{2+}$ ion-exchange process would be faster and most of the precipitation would occur outside the membrane. On the contrary, experimental results show that when using reducer concentrations above $3.75 \times 10^{-4} \text{ mol cm}^{-3}$, the platinum salt is totally precipitated in the membrane. Therefore, it can be assumed that the rate of precipitation is fast compared to the rate of mass transport. This means that the reaction ends when at least one of the two reactants (BH_4^- or $[\text{Pt}(\text{NH}_3)_4]^{2+}$) is exhausted. This is an approximation and additional work is needed to determine the rate law governing the reduction process. To take into account possible slower reactions, we used an empirical factor, τ , varying from 1 to 0 which limits the amount of platinum reduced in the presence of BH_4^- . $\tau = 1$ means that the reduction is fast and stops only when one or both of the two reactants are exhausted.

It is difficult to tell whether the rate of precipitation is controlled by an F or M mechanism. At significant reducer concentration, the limitation is certainly of the M-type [8]. But for lower concentrations, the F mechanism may be rate-determining. But for such concentrations, it can be argued that the hydrogen bubbles produced by the reduction process perturb the diffusion layer adjacent to the membrane surface and that the M mechanism prevails. Here it is assumed that the rate of precipitation is controlled by mass transport within the membrane.

3.3. Description of the model and hypotheses

The membrane sheet is represented in cross-section across its thickness, e (Fig. 3). The membrane (a $[\text{Pt}(\text{NH}_3)_4]^{2+}$ totally exchanged Nafion[®] 117 sample) was immersed at room temperature in a reducing solution of sodium borohydride.

The concentration profiles of the diffusing species along the x -axis, $C_i(x, t)$, were obtained under the following assumptions:

(i) The reducer concentration in the solution is sufficiently high and the chemical reduction is sufficiently

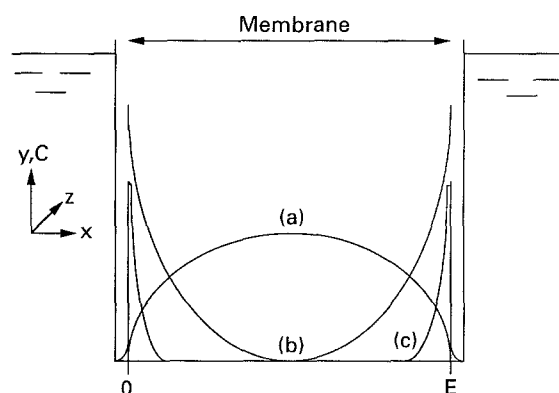


Fig. 3. Cross-section through the EME unit at a given time t . C_i concentration profiles are plotted across the membrane thickness: (a) $[\text{Pt}(\text{NH}_3)_4]^{2+}$, (b) Na^+ and (c) Pt^0 .

fast to assume that the kinetics of reduction are limited by mass transport within the membrane.

(ii) The bulk concentrations in solution are assumed to be time independent. Thus,

$$C_{\text{Na}^+} = C_{\text{BH}_4^-} = C^{\text{ste}} = C_{\text{b}}^0 \quad (1)$$

$$C_{[\text{Pt}(\text{NH}_3)_4]^{2+}} = 0 \quad (2)$$

This assumption holds when a sufficiently large volume of solution and sufficient stirring are used.

(iii) Concentrations in Na^+ and BH_4^- at the membrane-solution interface are given by the Donnan equation and remain constant throughout the precipitation.

(iv) It is assumed that interfacial equilibrium is independent of the interfacial fluxes as shown in [13].

(v) No water flux is associated with the ionic fluxes. The amount of water incorporated into the membrane during the pretreatment remains constant [14].

(vi) The amine groups produced by the reduction of $[\text{Pt}(\text{NH}_3)_4]^{2+}$ are not considered here since they are neutral entities.

(vii) The platinum tetramine which is not precipitated inside the membrane is not considered here. Its precipitation occurs only at the surfaces. The membrane surfaces are uniformly covered with a thin platinum layer used for electrical contact [6].

(viii) D_i are constant during the precipitation, and independent of the species concentration.

3.4. Model equations

The functions $C_i(x, t)$ are given by solution of the following set of equations:

$$\Phi_i = -D_i \frac{\partial C_i}{\partial x} - \frac{D_i z_i}{RT} F C_i \frac{\partial \phi}{\partial x} \quad (3)$$

$$\frac{\partial C_i}{\partial t} = -\frac{\partial \Phi_i}{\partial x} \quad (4)$$

$$\sum_i z_i C_i = 0 \quad \forall(x, t) \quad (5)$$

$$\sum_i z_i \Phi_i = 0 \quad \forall(x, t)$$

where i stands for Na^+ , BH_4^- and $[\text{Pt}(\text{NH}_3)_4]^{2+}$.

Equation 3 is the so-called Nernst-Planck flux equation in which the gradient of concentration and the electric potential are the driving forces. In deriving Equation 3, the following two assumptions are made: (a) that activities are approximated by concentrations, and (b) that absolute ionic mobilities and diffusion coefficients are related through the Einstein relation: $D_i = u_i kT$.

Equation 4 is the continuity equation which states that, in the absence of any ionic source or sink, mass is preserved.

Equation 5 is the electroneutrality condition. It may seem contradictory to assume that electroneutrality holds true at each (x, t) point in the membrane and to conserve an electric term in Equation 3. In fact, the electroneutrality Equation 5 may be taken as a

good approximation of Poisson's equation as the charge distribution in the membrane, although not zero, is small [15].

A reaction term of the form $\partial C/\partial t|_{\text{react}}$ was added to the platinum and borohydride flux equations to account for the chemical reduction. At each time step, the computed $C_{\text{Pt}}(x)$ and $C_{\text{BH}_4}(x)$ values obtained from Equation 3 were compared and $C_{\text{Pt}}^0(x)$ was incremented by a factor $\min(C_{[\text{Pt}(\text{NH}_3)_4]^{2+}}(x), 9/4 C_{\text{BH}_4}(x))$ where min represents the minimum function. $C_{[\text{Pt}(\text{NH}_3)_4]^{2+}}(x)$ and $C_{\text{BH}_4}(x)$ were modified accordingly.

The corrective factor, τ , defined above was included in the calculations in the form $(\tau \partial C/\partial t|_{\text{react}})$ to account for different chemical rates of reduction. All the computations were made with $\tau = 1$, except when expressly indicated. τ was the only adjustable parameter used in the calculations.

The system to obtain the time dependent concentrations of the diffusive species is

$$\frac{\partial C_i}{\partial t} = D_i \frac{\partial^2 C_i}{\partial x^2} + \frac{D_i z_i F}{RT} \frac{\partial C_i}{\partial x} \frac{\partial \phi}{\partial x} + \frac{D_i z_i F}{RT} C_i \frac{\partial^2 \phi}{\partial x^2} \quad (6)$$

Setting $D_1 = D_{[\text{Pt}(\text{NH}_3)_4]^{2+}}$; $D_2 = D_{\text{BH}_4^-}$; $D_3 = D_{\text{Na}^+}$ then combining Equations 5 and 6 gives

$$\frac{\partial \phi}{\partial x} = \frac{RT}{F} \left[\frac{z_1 \frac{\partial C_1}{\partial x} (D_2 - D_1)}{C_1 (D_1 z_1^2 - D_2 z_1 z_2) + D_2 z_2^2 C^-} \right] \quad (7)$$

From Equation 7, Equation 8 is obtained by analytical derivation:

$$\frac{\partial^2 \phi}{\partial x^2} = \frac{RT}{F} \left[\frac{z_1 (D_2 - D_1) \left[\frac{\partial^2 C_1}{\partial x^2} (C_1 D_1 z_1^2 - C_1 D_1 z_1 z_2 + C^- D_2 z_2^2) - z_1 \left(\frac{\partial C_1}{\partial x} \right)^2 (D_1 z_1 - D_2 z_2) \right]}{[C_1 D_1 z_1^2 - C_1 D_1 z_1 z_2 + C^- D_2 z_2^2]^2} \right] \quad (8)$$

3.5. Boundary limit conditions

The boundary conditions were set as follows (Donnan conditions):

$$(i) \quad C_{[\text{Pt}(\text{NH}_3)_4]^{2+}}(x=0, t) = 0 \quad (9)$$

$$(ii) \quad C_{\text{Na}, \text{M}}(x=0, t) = \frac{C^-}{2} + \sqrt{\left(\frac{C^-}{2}\right)^2 + (C_{\text{b}}^0)^2} \quad (10)$$

$$(iii) \quad C_{\text{BH}_4, \text{M}}(x=0, t) = \frac{(C_{\text{b}}^0)^2}{\sqrt{\left(\frac{C^-}{2}\right)^2 + (C_{\text{b}}^0)^2 + \frac{C^-}{2}}} = \frac{(C_{\text{b}}^0)^2}{C_{\text{Na}, \text{M}}(x=0, t)} \quad (11)$$

3.6. Treatment and solutions to the model

Solutions for $C_i(x, t)$ were obtained numerically. First

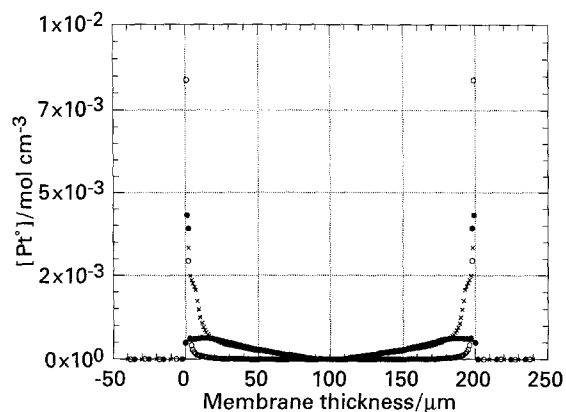


Fig. 4. Calculated platinum concentration profile across the membrane thickness using different NaBH_4 solutions: (○) $7.5 \times 10^{-5} \text{ mol cm}^{-3}$, (●) $3.75 \times 10^{-4} \text{ mol cm}^{-3}$ and (×) $1.0 \times 10^{-3} \text{ mol cm}^{-3}$.

and second order derivatives were approximated using the finite difference method. Local variations in metallic platinum concentration were computed at each iteration step and summed until the precipitation was complete.

Adjustment of the grid was obtained by comparison of the analytical and numerical solutions obtained in a simple case, in the absence of electric field, using the first order Fick diffusion equation. It was also checked, in each case, that the amount of platinum salt precipitated in the membrane added to the amount of the salt ion-exchanged with the solution was equal to the amount of salt initially in the membrane.

The metallic platinum concentration profile across

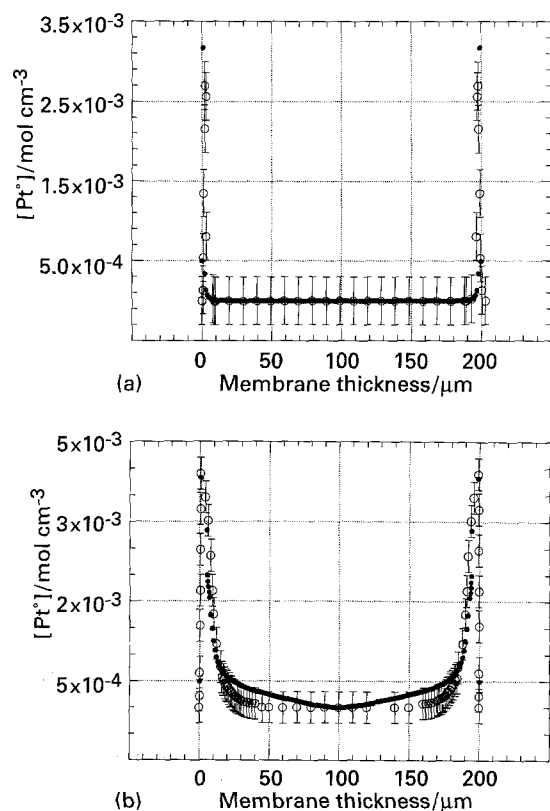


Fig. 5. Experimental (○) and calculated (●) platinum concentration profiles obtained for two reducer concentrations: (a) $7.5 \times 10^{-5} \text{ mol cm}^{-3}$, (b) $1.0 \times 10^{-3} \text{ mol cm}^{-3}$. $\tau = 1$.

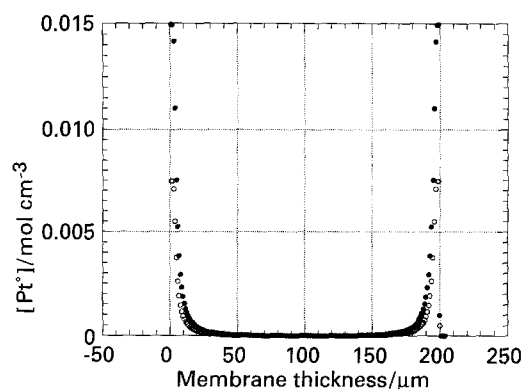


Fig. 6. Calculated platinum concentration profiles obtained after 1 and 2 loading-precipitation cycles. Reducing conditions: $[\text{NaBH}_4] = 7.5 \times 10^{-5} \text{ mol cm}^{-3}$ for 2 h, $\tau = 1$. Key: (○) 1 and (●) 2 cycles.

the membrane for different reducer concentrations are shown in Fig. 4. Precipitation is seen to occur preferentially at the membrane surfaces as observed experimentally. The distribution of platinum clusters depends very markedly upon the reducer concentration.

The effect of the following parameters was studied:

- (i) concentration C_b^0 in reducer in the solution, $2.5 \times 10^{-5} < C_b^0 < 2 \times 10^{-3} \text{ mol}^{-3}$
- (ii) diffusion coefficient of the diffusing species Na^+ , $[\text{Pt}(\text{NH}_3)_4]^{2+}$ and BH_4^-
- (iii) number of successive loading-precipitation cycles (from 1 to 4)
- (iv) reactivity of $[\text{Pt}(\text{NH}_3)_4]^{2+}$ and NaBH_4 expressed by the factor τ .

4. Results and discussion

4.1. Verification of the model

Experimental and calculated concentration profiles obtained using two different reducer concentrations are shown in Fig. 5. After normalization of the experimental data as indicated in the experimental section, good agreement is found between experimental and calculated values.

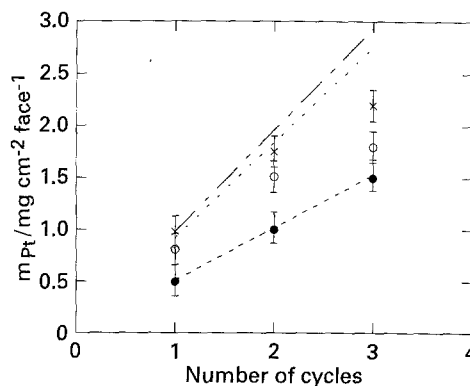


Fig. 7. Platinum loading (in mg cm^{-2} per face) against the number of successive loading-precipitation cycles. Comparison of experimental and computed (dashed lines) results obtained from different reducer concentrations in solution: (●) $7.5 \times 10^{-5} \text{ mol cm}^{-3}$; (○) $3.75 \times 10^{-4} \text{ mol cm}^{-3}$; (×) $1.0 \times 10^{-3} \text{ mol cm}^{-3}$. $\tau = 1$.

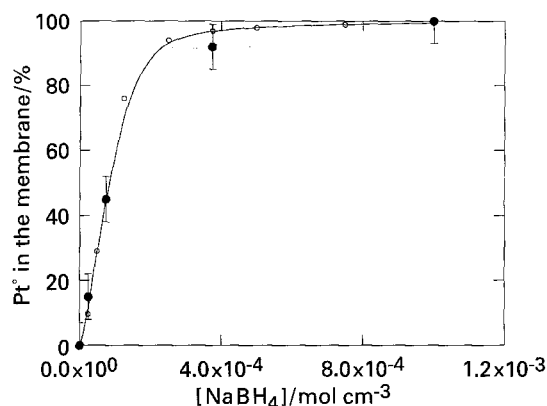


Fig. 8. Determination of the amount of platinum precipitated in the membrane as a function of the reducer concentration in the solution. Comparison of measured (●) and calculated (○) data.

Calculated data obtained after one and two loading-precipitation cycles are shown in Fig. 6. For low surface concentrations, the fit is good (Fig. 7). But since, in the model, no restriction was introduced on the maximum value of local platinum concentration, experiment and theory differ when the membranes become heavily loaded with solid particles. For such cases, a change in the value of the diffusion coefficient has to be considered.

The amount of metallic platinum reduced within, and at, the surface of the membrane depends markedly upon the reducer concentration in the solution (Figs 8 and 9). The higher the concentration, the lower the amount of platinum lost by precipitation in the solution. But at high salt concentrations (above ca. $3.75 \times 10^{-4} \text{ mol cm}^{-3}$), the precipitation also occurs in the bulk membrane. Isolated metallic clusters, useless for the electrochemical process, are formed across the entire membrane thickness. Therefore, an optimal value of the reducer concentration has to be found, for a given hydrodynamic regime. An empirical value of $7.5 \times 10^{-5} \text{ mol cm}^{-3}$ was determined in an earlier work [7]. The same value is obtained here by calculation.

Figure 10 shows the calculated curves obtained for two different chemical reactivities ($\tau = 1$ and $\tau = 0.1$). It can be seen that a change in chemical reactivity does not significantly change the shape of the profiles though the amount of platinum precipitated in the

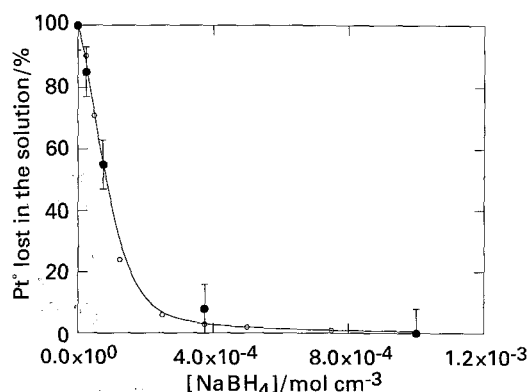


Fig. 9. Determination of the amount of platinum precipitated in the solution as a function of the reducer concentration in the solution. Comparison of measured (●) and calculated (○) data.

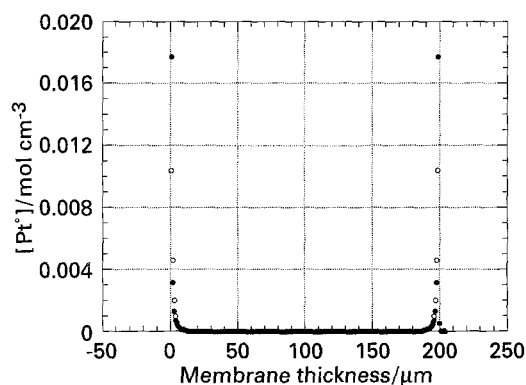


Fig. 10. Calculated curves obtained with a $7.5 \times 10^{-5} \text{ mol cm}^{-3}$ NaBH₄ solution. Effect of different chemical reactivities: (●) $\tau = 1$ and (○) $\tau = 0.1$.

membrane is significantly different (49% with $\tau = 1$ and 39% with $\tau = 0.1$).

4.2. Sensitivity of the model

$$\text{Setting: } \Sigma = 1000 M_{\text{Pt}^0} \frac{V}{e} \int_0^e C_{\text{Pt}^0} dx \quad (12)$$

the sensitivity of the model to the different parameters controlling the precipitation can be measured by calculating the relative change in Σ as a function of the relative change in each of these parameters. C_b^0 (the reducer concentration), $D_{[\text{Pt}(\text{NH}_3)_4]^{2+}}$ (platinum diffusion coefficient), and $D_{\text{BH}_4^-}$ (borohydride diffusion coefficient) turned out to play a significant role (Fig. 11). Values of the parameters chosen for the reference case in Fig. 11 are shown in Table 1.

5. Conclusions

Using phenomenological mass-transport equations, the metallic platinum concentration profiles across the membrane have been computed. The calculated data compare well with experimental data obtained by electron microprobe analysis. The model shows the effect of the reducer concentration and the number of successive loading-precipitation cycles. Adequate Pt-based SPE[®] composites, that is,

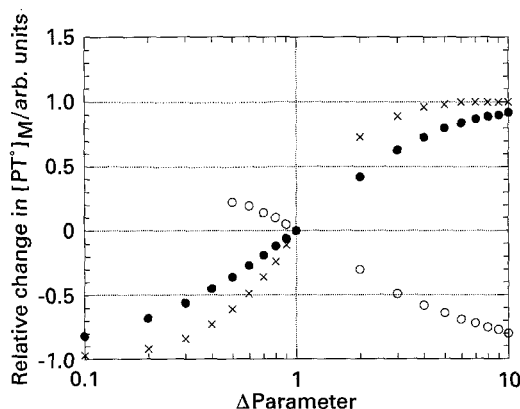


Fig. 11. Sensitivity of the model. Plots of the relative change in Σ ($\text{mg Pt}^0 \text{ cm}^{-2}$ per face), as a function of $D_{[\text{Pt}(\text{NH}_3)_4]^{2+}}$ (○), $D_{\text{BH}_4^-}$ (●) and C_b^0 (×).

Table 1. Values of the parameters used for the reference case of Fig. 11

$[\text{NaBH}_4] = 7.5 \times 10^{-5} \text{ mol cm}^{-3}$	$C^- = 10^{-3} \text{ mol cm}^{-3}$
$D_{[\text{Pt}(\text{NH}_3)_4]^{2+}} = 5.2 \times 10^{-7} \text{ cm}^2 \text{ s}^{-1}$	$\tau = 1.0$
$D_{\text{BH}_4^-} = 5.0 \times 10^{-7} \text{ cm}^2 \text{ s}^{-1}$	$\Delta x = 1 \mu\text{m}$
$D_{\text{Na}^+} = 4.5 \times 10^{-6} \text{ cm}^2 \text{ s}^{-1}$	

Nafion[®] membranes loaded with two thin platinum electrodes localized near the membrane surfaces, are obtained using ca. $7.5 \times 10^{-5} \text{ mol cm}^{-3}$ NaBH₄ reducing solutions. With lower reducer concentrations, most of the platinum tetramine is precipitated in the solution and with higher reducer concentrations, most of the salt is lost by precipitation in the bulk membrane. Additional work is needed to determine the rate law governing the reduction process.

Concerning the sample size problem, the model shows that adequate platinum concentration profiles across the membrane are obtained when mass transport is limited by diffusion and migration inside the membrane. The preparation of samples larger than 5 cm² is usually achieved by using two-compartment plating cells. Special care must be given to the design of these cells, especially to achieve homogeneous fluid distribution over the membrane surface and to increase the fluid velocity so that mass transport is limited by diffusion in the membrane itself and not in the diffusion layer adjacent to the membrane surface.

While platinum based Nafion[®] composites are of interest for water electrolysis and hydrogen/oxygen fuel cells applications, the technique can be used for

the preparation of various other SPE[®] composites. For example, ruthenium or iridium oxide based anodes can be used in SPE[®] electrolyzers and ruthenium based anodes in SPE[®] brine electrolysis. Given adequate experimental data (diffusion coefficients, membrane characteristics, etc.), it is possible to predict the shape of the concentration profiles after reaction. The model can also be used to predict rates of ion-exchange and to model separation processes.

References

- [1] W. A. Titterington and J. F. Austin, 'Extended Abstract', ECS Fall Meeting, New York (1974) p. 576.
- [2] H. Takenaka, E. Torikai, Y. Kawami and N. Wakabayashi, *Int. J. Hydrogen Energy* **7** (1982) 397.
- [3] G. Scherer, H. Devantay, R. Oberlin and S. Stucki, 'Dechema Monographien', Band 98, Verlag Chemie, (1985) p. 407.
- [4] E. J. Taylor, E. B. Anderson and N. R. K. Vilambi, *J. Electrochem. Soc.* **139** (1992) L-45.
- [5] R. Durand, P. Millet and M. Pinéri, *French Patent 87 17 637* (1987).
- [6] *Idem*, *Int. J. Hydrogen Energy* **15** (1990) 245.
- [7] *Idem*, *J. Appl. Electrochem.* **19** (1989) 162.
- [8] P. Millet, R. Durand, E. Dartyge, G. Tourillon and A. Fontaine, *J. Electrochem. Soc.* **140** (1993) 1373.
- [9] P. Millet, F. Andolfatto and R. Durand, *J. Appl. Electrochem.*, submitted.
- [10] P. Millet, *J. Membrane Sci.* **50** (1990) 325.
- [11] A. Michas, PhD thesis, Grenoble (1986).
- [12] P. Van Rheezen, M. McKelvy, R. Marzke and W. S. Glaunsinger, *Trans. Met. Comp. & Complexes* (1983) 238.
- [13] C. Selvey and H. Reiss, *J. Membrane Science* **30** (1987) 75.
- [14] H. Takenaka, E. Torikai, Y. Kawami and N. Wakabayashi, Proceedings of the 3rd World Hydrogen Energy Conference, Tokyo (1980) p. 107.
- [15] A. D. McGillivray, *J. Chem. Phys.* **48** (1968) 2903.